Magnetoelastic coupling in [Ru_{2}(O_{2}CMe)_{4}]_{3}[Cr(CN)_{6}] molecule-based magnet

T. V. Brinzari, P. Chen, L. -C. Tung, Y. Kim, D. Smirnov, J. Singleton, Joel. S. Miller, and J. L. Musfeldt

Phys. Rev. B **86**, 214411 — Published 14 December 2012

DOI: 10.1103/PhysRevB.86.214411

Magnetoelastic coupling in $[Ru_2(O_2CMe)_4]_3[Cr(CN)_6]$ molecule-based magnet

T. V. Brinzari,[1] P. Chen,[1] L. -C. Tung,[2,*] Y. Kim,[2] D. Smirnov,[2] J. Singleton,[3] Joel. S. Miller,[4] and J. L. Musfeldt[1]

[1]*Department of Chemistry, University of Tennessee, Knoxville, Tennessee 37996, USA*
[2]*National High Magnetic Field Laboratory, Tallahassee, Florida 32310, USA*
[3] *National High Magnetic Field Laboratory, Los Alamos National Laboratory, Los Alamos, New Mexico 87545, USA*
[4]*Department of Chemistry, University of Utah, Salt Lake City, Utah 84112, USA*

Infrared and Raman vibrational spectroscopies were employed to explore the lattice dynamics of $[Ru_2(O_2CMe)_4]_3[Cr(CN)_6]$ through the field- and temperature-driven magnetic transitions. The high field work reveals systematic changes in the C≡N stretching mode and Cr-containing phonons as the system is driven away from the antiferromagnetic state. The magnetic intersublattice coalescence transition at B_c≃0.08 T, on the contrary, is purely magnetic and takes place with no lattice involvement. The variable temperature spectroscopy affirms overall $[Cr(CN)_6]^{3-}$ flexibility along with stronger intermolecular interactions at low temperature. Based on a displacement pattern analysis, we discuss the local lattice distortions in terms of an adaptable chromium environment. These findings provide deeper understanding of spin-lattice coupling in $[Ru_2(O_2CMe)_4]_3[Cr(CN)_6]$ and may be useful in the development of technologically important molecule-based magnets.

PACS numbers: 75.50.Xx, 63.70.+h, 75.30.Kz, 75.80.+q

I. INTRODUCTION

Molecule-based materials offer unique opportunities to investigate the interplay between charge, structure, and magnetism and for an understanding of multifunctional behavior at the microscopic level.[1–3] The rich variety of molecular components, the flexibility of molecular frameworks, and the overall low energy scales are particularly attractive for the design of materials with controllable and tunable magnetic properties.[4,5] For a molecule-based magnet in which superexchange between metal ions relies on diamagnetic ligand linkages, the interplay between spin and lattice degrees of freedom can be an important aspect for ground state stabilization.[6–8] Moreover, coupling often impacts how a particular state can be tuned with pressure, temperature, magnetic field, or chemical substitution.[7–11] $[Ru_2(O_2CMe)_4]_3[Cr(CN)_6]$ (Me=CH_3) attracted our attention due to its interpenetrating magnetic networks, novel spin structure, metamagnetic transition, and predicted high field spin-flop.[10,12–15] These attributes combine to make this material well suited to extended investigations of magnetoelastic coupling.

$[Ru_2(O_2CMe)_4]_3[Cr(CN)_6]$ has a body-centered cubic structure (space group $Im\bar{3}m$) with two identical interpenetrating lattices (Fig. 1). A single sublattice consists of alternating $[Ru_2(O_2CMe)_4]^+$ and $[Cr(CN)_6]^{3-}$ units with Cr^{III} ions residing at the corners of the cubic unit cell (a=13.376 Å) and linked by CN-bridges to $Ru_2^{II/III}$ dimers at the twelve cubic edges (Fig. 1(a, b)).[12,16] The second sublattice resides in the open space of the first sublattice (Fig. 1(c)). Each Cr^{III} center of $[Cr(CN)_6]^{3-}$ and each mixed-valent $Ru_2^{II/III}$ unit of $[Ru_2(O_2CMe)_4]^+$ has a spin S=3/2.[17] A large easy-plane anisotropy D≃8.6 meV (69 cm^{-1}) is associated with the $[Ru_2(O_2CMe)_4]^+$ paddle wheel complex.[16] Below the 33 K ordering temperature, the system displays antiferromagnetic (AFM) intrasublattice coupling J_c≃1.5 meV (12 cm^{-1}) between neighboring Cr^{III} ion and net $Ru_2^{II/III}$ dimer moments, resulting in a ferrimagnetic arrangement of each sublattice and a weak AFM intersublattice coupling K_c≃5×10^{-3} meV (0.04 cm^{-1}).[15] A modest magnetic field (B_c≃0.08 T) aligns the moments on each sublattice.[14] This is a type of metamagnetic transition between AFM and paramagnetic (PM) states in which sublattices magnetically coalescence. Theoretical calculations also predict a spin-flop transition at B_{sf}≃80 T, and even higher magnetic fields should drive

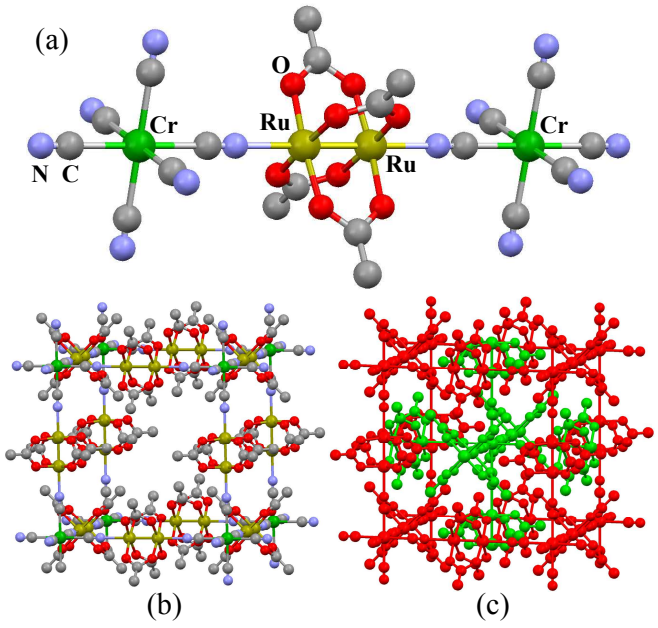

FIG. 1: (Color online) (a) Cr^{III}-$Ru_2^{II/III}$-Cr^{III} structural linkage along with (b) the single, non-interpenetrating sublattice, and (c) a diagram of the two interpenetrating lattices (red and green) in body-centered cubic $[Ru_2(O_2CMe)_4]_3[Cr(CN)_6]$.[12,16] Hydrogens are omitted for clarity.

the system to the fully polarized state.[15] At this stage, however, no experimental work at high magnetic fields has been done, so our investigations bring additional insight to the behavior of $[Ru_2(O_2CMe)_4]_3[Cr(CN)_6]$ in this regime. Pressure collapses the magnetic coalescence transition and reveals an effective $Ru_2^{II/III}$ high-spin $\rightarrow$ low-spin transition,[10,18] thus providing additional evidence for rich and tunable magnetoelastic interactions in this system.

In this work, we combine high field and variable temperature spectroscopies to probe spin-lattice interactions in the $[Ru_2(O_2CMe)_4]_3[Cr(CN)_6]$ molecule-based magnet. In applied field, correlation between the measured vibrational response, the displacement patterns, and local lattice distortions reveals magnetoelastically-active $[Cr(CN)_6]^{3-}$ octahedral units and rigid $[Ru_2(O_2CMe)_4]^+$ paddle wheel dimers as the system is driven away from the AFM ground state. At the same time, variable temperature studies show pronounced changes in modes connected with the $[Cr(CN)_6]^{3-}$ octahedra, demonstrating the overall softness of this moiety and its readiness to adapt to a new physical environment. Taken together, our analysis reveals the key local lattice distortions that underpin magnetoelastic properties of this system under applied magnetic field. These findings have implications for other cyanide-bridged complexes like Prussian blue structure materials of $M_x[M(CN)_6]_y$ composition or Cr-containing oxides where similar mechanisms may be important.[11,19,20]

II. METHODS

Polycrystalline $[Ru_2(O_2CMe)_4]_3[Cr(CN)_6]$ was prepared as described previously.[12] Magnetization measurements were performed at the National High Magnetic Field Laboratory (NHMFL) using a 60 T short-pulse magnet at several different temperatures.[21] Spectroscopic work was carried out on pressed powder samples mixed with transparent matrix material (paraffin, KCl) or pure powder. All samples displayed some degree of the decomposition, although without detriment to the bulk magnetic properties – either in previous work or in our own measurements. Special care was required, however, for the spectroscopic studies. We found, for instance, that in an alkali halide environment, pressure increases the decomposition rate. This was evident from the appearance of broad infrared absorption lines at 1550 cm^{-1} and near 2080-2090 cm^{-1}.[22] Several efforts were made to minimize these effects and access the intrinsic spectral response. As an example, magnetic field- and temperature-dependent behavior of the CN vibration near 2145 cm^{-1} was checked in an unconventional arrangement (employing a paraffin matrix) and after appropriate background subtraction, found to be consistent with the KCl pellet response. Moreover, the signature vibrational bands of the decomposition-induced defect states were found to be magnetically inactive. Magneto-infrared and magneto-Raman ($\lambda_{exc} = 532$ nm, $\simeq$1.5 mW) work was carried out at the NHMFL using a water-cooled DC magnet (0–35 T, 4.2 K). Complementary variable temperature spectroscopy was performed between 10 and 300 K. Spectral resolution of 0.5-1 cm^{-1} was employed depending on the experiment. The infrared absorption coefficient $\alpha(\omega)$ was calculated as $\alpha(\omega) = -\frac{1}{hd}\ln(T(\omega))$, where h is the pellet concentration and d is the thickness. Standard fitting techniques were employed as appropriate.

III. RESULTS AND DISCUSSION

A. Lattice dynamics through the metamagnetic transition and towards the high field state

The 4.2 K far infrared absorption spectrum of $[Ru_2(O_2CMe)_4]_3[Cr(CN)_6]$ in zero field is shown in Fig. 2(a) along with the full field absorption difference $\Delta\alpha = \alpha(B = 35\text{ T}) - \alpha(0\text{ T})$. The latter highlights the field-induced spectral changes clearly demonstrating the sensitivity of certain modes to magnetic field and the rigidity of others. Figure 2(b) illustrates the systematic development of features near 370 and 460 cm^{-1}. Investigation of the higher frequency response (up to 3200 cm^{-1}) reveals only one additional feature near 2145 cm^{-1} that is affected by external field (Fig. 2(c)). All other infrared-active phonons remain rigid. We interpret these findings in terms of field-induced local lattice distortions.[23]

Assignment of the spectral peaks allows us to transform our findings into an understanding of local structural deformations. Group theory predicts four F_{1u} infrared-active vibrations for a $[Cr(CN)_6]^{3-}$ block of an ideal octahedral environment. Previous studies of $[M(CN)_6]^{n-}$-based compounds identified these frequencies as 90-160, 340-350, $\simeq$460 and 2120-2130 cm^{-1}.[24–27] Bringing these literature data together with our independent measurements of model compounds like $K_3[Cr(CN_6]$, we assign the $[Ru_2(O_2CMe)_4]_3[Cr(CN)_6]$ bands near 120, 370, 460, 2145 cm^{-1} to the δ(C-Cr-C) bend, ν(Cr-C) stretch, δ(Cr-C-N) bend, and ν(C$\equiv$N) stretch, respectively.[28] The strong peak at $\simeq$400 cm^{-1} is assigned as a ν(Ru-O) stretch.[29,30] This assignment agrees with frequency and intensity variations in metal-substituted $[Ru_2(O_2CMe)_4]_3[M^{III}(CN)_6]$ (M = Fe, Co) and also the $[Ru_2(O_2CMe)_4]Cl$ parent compound.[31]

Combining mode assignment and displacement pattern information with the magneto-infrared spectra, it is apparent that applied field dominantly affects the octahedral $[Cr(CN)_6]^{3-}$ centers (as evidenced by the sensitivity of the 120, 370, 460 and 2145 cm^{-1} peaks) and barely perturbs modes emanating from the $[Ru_2(O_2CMe)_4]^+$ paddle wheel complex. Interestingly, the response is not the same for each mode, even though all, except for the C$\equiv$N stretch, involve the Cr^{III} ion. Detailed views of the absorption difference spectra (Fig. 2(a, b, c)) clearly illustrate these features. The 120 cm^{-1}

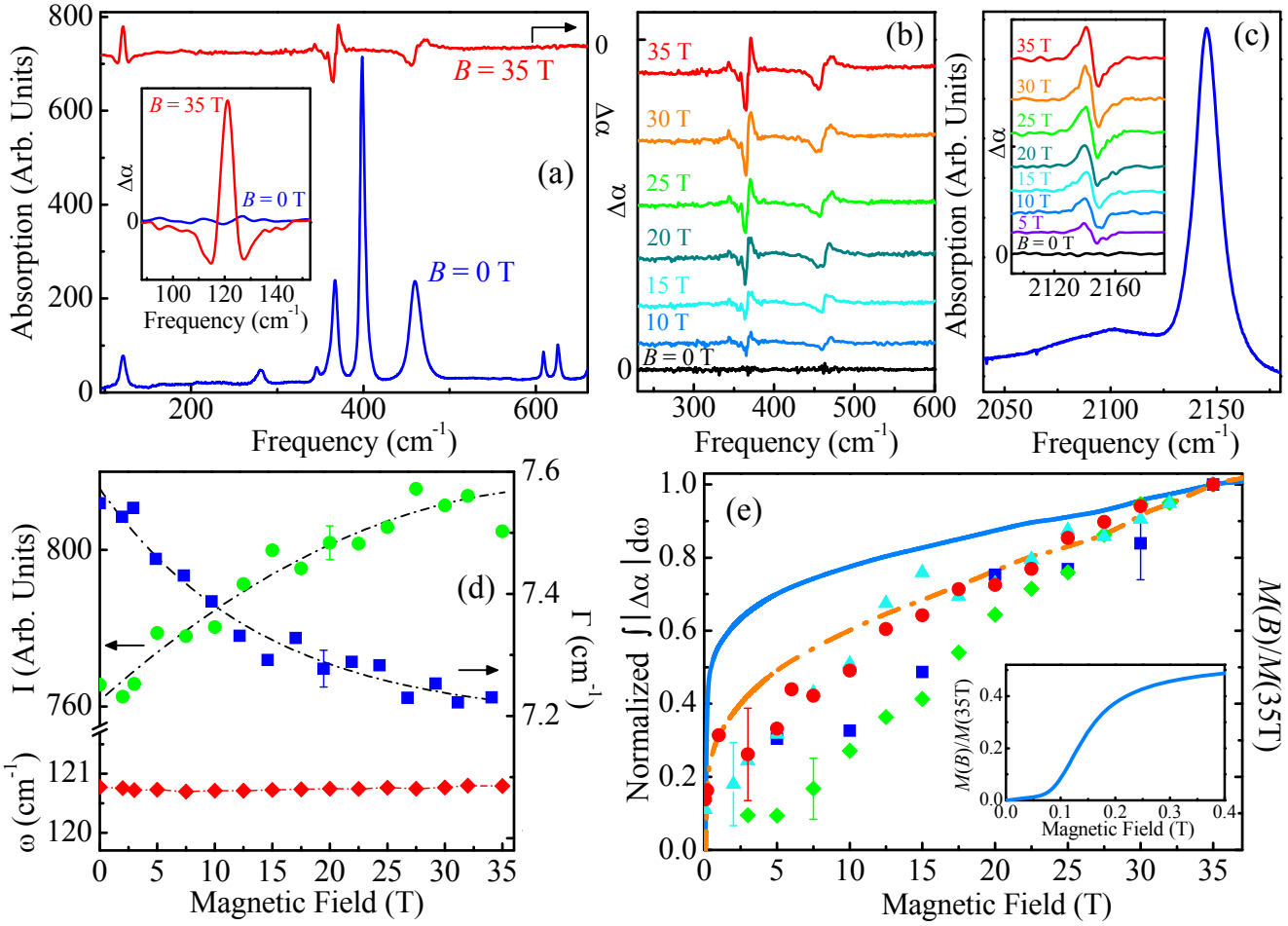

FIG. 2: (Color online) (a) Far infrared absorption spectrum of $[Ru_2(O_2CMe)_4]_3[Cr(CN)_6]$ at $B = 0$ T along with the full field absorption difference spectrum $\Delta\alpha = \alpha(B = 35\text{ T}) - \alpha(0\text{ T})$. Inset: Close-up view of $\Delta\alpha = \alpha(B) - \alpha(0\text{ T})$ at $B = 0$ and 35 T for the $\simeq$120 cm^{-1} phonon emphasizing its different shape as compared to the other features. The $B = 0$ T curve demonstrates the sensitivity level of $\Delta\alpha$ calculated using scans before and after the field sweep. (b) $\Delta\alpha$ of the 370 and 460 cm^{-1} modes at representative fields highlighting their vibrational contrast. Data are offset for clarity from the $B = 0$ T curve. (c) Absorption profile of the ν(C$\equiv$N) stretch at 2145 cm^{-1} along with the corresponding field-induced changes in $\Delta\alpha$ (inset). Data are offset for clarity. (d) Intensity (I), frequency (ω), and linewidth (full width at half maximum, Γ) as a function of field for the δ(C-Cr-C) bend near 120 cm^{-1}. Lines guide the eye. (e) Integrated absolute absorption difference vs. applied field compared with the magnetization and the square of the magnetization. The data are normalized to 35 T. (—) - 4 K magnetization ($M(B)$), (—) - $(M(B))^2$, ▲ - 120 cm^{-1}, ♦ - 370 cm^{-1}, ■ - 460 cm^{-1} and ● - 2145 cm^{-1} peaks. All magneto-infrared data were collected at 4.2 K. Inset: Close-up view of low field magnetization demonstrating the magnetic intersublattice coalescence transition at $B_c\simeq$0.08 T. Magnetization measurements up to 60 T do not reveal any additional transitions.

mode is characterized by a sharp peak centered between two minima whereas the 370, 460 and 2145 cm^{-1} features have derivative-like structures. The former lineshape is characteristic of field-induced width and intensity changes, whereas the derivative-like lineshape points to field-induced frequency shifts (with both red and blue shifts observed in $[Ru_2(O_2CMe)_4]_3[Cr(CN)_6]$). Here and elsewhere in the text, "softening" or "red shifting" indicates a shift to lower energy, whereas "hardening" or "blue shifting" refers to a shift to higher energy.

In general, peak position, linewidth, and intensity trends are sensitive indicators of phase transition mechanisms.[32–34] These quantities are particularly useful for revealing magnetoelastic interactions through field-driven transitions.[8,35,36] As an example, Fig. 2(d) shows the gradually increasing intensity and the simultaneously decreasing linewidth of the 120 cm^{-1} phonon. The peak position remains constant, and total oscillator strength is approximately conserved. This behavior suggests a gradual field-induced reduction of the damping constant (Γ) for the δ(C-Cr-C) vibration. We find $|\Delta\Gamma|/\Gamma(0\text{ T}) = (\Gamma(35\text{ T}) - \Gamma(0\text{ T}))/\Gamma(0\text{ T}) \approx 4 \pm 0.5\%$.

To reveal trends in the higher frequency phonons, we integrate the absolute value of the absorption difference spectrum as $\int_{\omega_1}^{\omega_2} |\Delta\alpha|\, d\omega = \int_{\omega_1}^{\omega_2} |\alpha(B) - \alpha(0\text{ T})|\, d\omega$ (where ω_1 and ω_2 define the frequency range of interest),

and plot these data as a function of magnetic field.[37] The low temperature magnetization ($M(B)$) and the square of the magnetization ($(M(B))^2$) are included for comparison (Fig. 2(e)). The magnetization data are characterized by a fast initial rise at low fields that is a signature of the intersublattice coalescence transition,[12,14] followed by a continuous rise at higher fields as the field slowly overtakes the system anisotropy and exchange interactions.[15,16] Within our sensitivity, there is no magneto-infrared contrast through the magnetic coalescence transition. The lack of change in the infrared spectrum at $B_c \simeq 0.08$ T, the field where both sublattice moments become aligned, indicates little spin-lattice interaction and a rigid lattice through the magnetic intersublattice coalescence. This finding may be useful for understanding magneto-structural correlations in other metamagnetic materials[38–40] in that modeling efforts can focus on spin-only interactions.

Above B_c, the field slowly cants spins away from AFM alignment in competition with the intrasublattice exchange interactions and ruthenium anisotropy.[15] At the same time, there is clear evidence of magnetoelastic interactions in the form of field-dependent phonons (Fig. 2), and as in the case of $Mn[N(CN)_2]_2$,[36] the magneto-infrared response seems to have a better match with $(M(B))^2$ rather than the magnetization itself. This suggests the exchange nature of the magnetoelastic effect.[41] Using $|\Delta\alpha|/\alpha = |\alpha(35\ \mathrm{T}) - \alpha(0\ \mathrm{T})|/\alpha$ to quantify the coupling for each type of displacement, we find that the most prominent change, of the order of 2-3%, can be attributed to softening of the C≡N stretching mode. The ν(Cr-C) stretch and the δ(Cr-C-N) bend show slightly smaller changes, 1-2% and 1%, respectively. Both modes harden in field. The magnetic energy scales in $[Ru_2(O_2CMe)_4]_3[Cr(CN)_6]$ allow us to probe only the onset of the spin-lattice interactions. More pronounced effects are anticipated at higher fields.

The finding of flexible CrC_6 octahedra and relaxed C≡N linkages in $[Ru_2(O_2CMe)_4]_3[Cr(CN)_6]$ at high fields can be correlated with the crystal structure (Fig. 1) in which the CN ligands bridge the Cr^{III} and $Ru_2^{II/III}$ magnetic centers providing an effective superexchange pathway.[12] When field competes with superexchange interactions (with energy scale J_c), the process is accompanied by magnetoelastic interactions in which the chromium environment and in particular the bridging CN units distort to accommodate the developing magnetic state.[42] Similar cooperative effects occur in other materials.[8,36,43] From the direction of the field-induced blue shift of Cr-containing phonons and a simple "frequency-bond distance" correlation,[44,45] the high field local geometry likely consists of a compressed CrC_6 octahedron. There is no evidence for octahedral distortion within our sensitivity, so we conclude that the compression is isotropic, although this finding should be tested at higher fields.[46] In case of the CN linkages, softening points to an overall more relaxed environment of this unit. The relationship to the bond length however, is more complex and an inverse correlation is indicated as discussed below.

To complement our high field work on ungerade symmetry vibrations, we investigated the magneto-Raman response of $[Ru_2(O_2CMe)_4]_3[Cr(CN)_6]$ with particular interest in the symmetric Ru-Ru and Ru-O modes. Our low temperature Raman spectrum reveals two strong lines near 320 and 360 cm^{-1} and a number of weaker, broader structures whose low intensity precludes detailed investigation. Here, we focus our discussion on two intense features near 320 and 360 cm^{-1}. Based on literature data and the insensitivity of these lines to M^{III} (M=Cr, Co, Fe) substitution, we assign them as Ru-Ru and Ru-O stretching bands, respectively.[29] Application of a 35 T field reveals no changes in the behavior of these modes within our sensitivity, consistent with the magneto-infrared result of a rigid $[Ru_2(O_2CMe)_4]^+$ cluster.

$[Cr(CN)_6]^{3-}$, and hexacyanometalates in general, are attractive and oft-used molecular building blocks.[5,11,47,48] The chemical diversity of polycyanide molecular precursors combined with the tunability of their magnetic properties through flexible M-CN-M linkages led to materials with room temperature and photoinduced magnetism, metamagnetism, spin-crossover, and charge transfer induced transitions.[11,38,47,49–52] The magnetoelastic interactions revealed in $[Ru_2(O_2CMe)_4]_3[Cr(CN)_6]$ bring additional understanding of magnetostructural correlations in the development of flexible magnetism and tunable properties in materials where the adaptable cyanide ligands provide important control paths for magnetic coupling between metal centers.

B. Vibrational response through the 33 K magnetic ordering transition

We already demonstrated that external stimuli like magnetic field in combination with vibrational spectroscopy can be used to reveal local lattice distortions. To gain additional insight into magnetoelastic coupling in $[Ru_2(O_2CMe)_4]_3[Cr(CN)_6]$, we examined the variable temperature infrared response. Figure 3(a) and (b) displays the full infrared spectrum. Modes that resonate at 116, 361, 449, and 2138 cm^{-1} harden significantly with decreasing temperature (300-10 K), with $\simeq$4, 6, 12, 7 cm^{-1} shifts, respectively. This is in contrast to trends in several other phonons, for example the 398 cm^{-1} mode, with a frequency shift on the order of 1 cm^{-1} (Fig. 3(c)). Moreover, frequency vs. temperature behavior is monotonic with no anomalies at or near the 33 K magnetic ordering transition (Fig. 3(d)). The latter suggests inherently weak spin-lattice coupling in this material that can be amplified and/or revealed by driving the system towards a collective transition using external magnetic field. Similar effects are of interest in oxides.[53]

Temperature and magnetic field are often considered

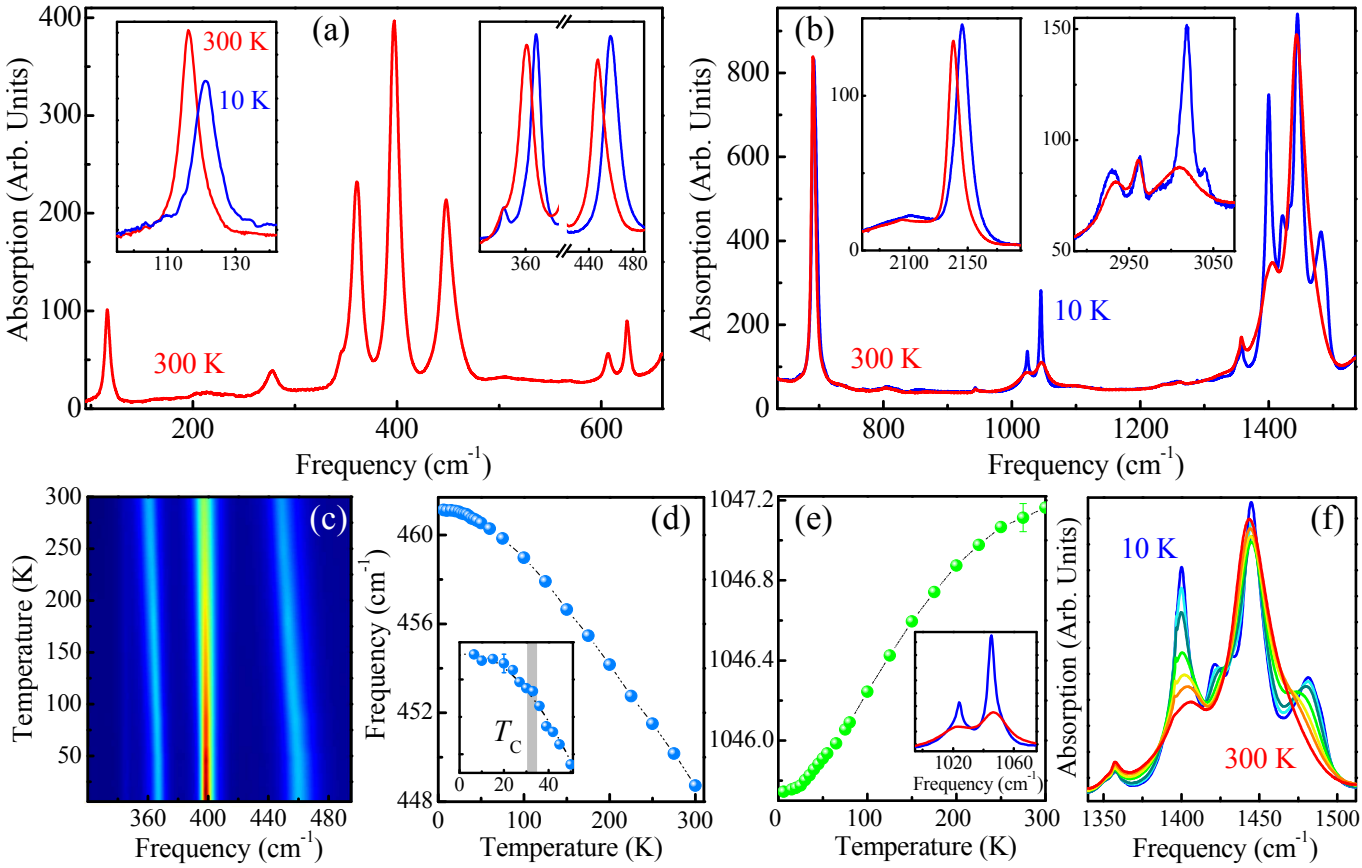

FIG. 3: (Color online) (a) The far infrared spectrum of $[Ru_2(O_2CMe)_4]_3[Cr(CN)_6]$ at 300 K. Inset (left): Close-up view of the low frequency δ(C-Cr-C) deformation mode at 300 and 10 K. Inset (right): Close-up view of the ν(Cr-C) and δ(Cr-C-N) modes emphasizing the pronounced frequency shifts between room temperature and 10 K. (b) Middle-infrared spectrum of the $[Ru_2(O_2CMe)_4]_3[Cr(CN)_6]$ molecular magnet at 300 and 10 K. Insets: Close-up view of the ν(CN) and ν(CH) stretching modes, respectively. (c) Image plot of peak intensities as a function of frequency and temperature for the mode cluster near 400 cm^{-1}: blue - low intensity, red - high intensity. (d) and (e) Frequency vs. temperature trends for selected vibrational features with hardening and softening behavior, respectively. Inset (d): Close-up view of the systematic frequency variation through the 33 K transition temperature. Inset (e): Close-up view of the high and low temperature spectra near 1040 cm^{-1}. (f) Spectral evolution of the $\simeq$1450 cm^{-1} cluster at 10, 30, 50, 100, 150, 200 and 300 K.

to be complementary thermodynamic variables,[54] so similarities between the temperature and field behaviors are anticipated. Perhaps the most important of these relates to the $[Cr(CN)_6]^{3-}$ octahedra, which retain their role as flexible building blocks. This is consistent with the overall changes in Cr-C and C≡N bond lengths as compared with Ru-O, Ru-N, and Ru-Ru distances.[55] Interestingly, while hardening of ν(Cr-C) and δ(CrCN) bands is in line with a shorter Cr-C distance at 1.8 K, the blue shift of ν(CN) is in contrast to an elongated C≡N bond. Systems in which a "frequency-bond length" correlation breaks down are known, and we attribute the lack of a simple relationship to superimposed bond length, charge, intermolecular force, and collectivity effects.[36,45,56,57] In any case, the finding of thermally susceptible $[Cr(CN)_6]^{3-}$ units parallels the situation in magnetic field. Note however, that the overall vibrational behavior is not the same for all features (as seen from the frequency shift of ν(Cr-C) and δ(Cr-C-N) modes, for example), indicating that even a simple magnetocaloric effect that corresponds to adiabatic change in temperature due to field modification[54] cannot account for these trends. In addition to the frequency shift, the 120 cm^{-1} δ(C-Cr-C) bend also displays damping constant variations (inset, Fig. 3(a)) in line with our magnetic field studies. The broader low temperature linewidth in combination with diminished intensity is different than the conventional thermal response and may be indicative of phonon interaction with other excitations and/or states. Both temperature and magnetic field seem to suppress this interaction and decouple the phonon.

The $[Ru_2(O_2CMe)_4]_3[Cr(CN)_6]$ temperature dependence reveals several other trends. For instance, the features near 1045, 1400-1430, and 2930 cm^{-1}, soften down to 10 K (Fig. 3(e, f)), behavior that is opposite to normal lattice contraction tendencies.[55] In addi-

tion, the broad cluster of absorptions centered at 1450 cm^{-1} displays interesting fine structure due to simultaneous softening/hardening of the low/high frequency components.[58] Previous work on the $[Ru_2(O_2CMe)_4]_3Cl$ parent compound as well $Cu_2(O_2CMe)_4(H_2O)_2$ allows us to assign modes near 1025 and 1045 cm^{-1} to $\rho(CH_3)$ rocking, the cluster near 1450 cm^{-1} to $\delta(CH_3)$ deformations and $\nu(CO)_{sym/asym}$ stretches, and features centered at 2990 cm^{-1} as $\nu(CH_3)_{sym/asym}$ stretches.[29,59,60]

Given the nature of these modes and their displacement patterns, the pronounced changes in the 1450 cm^{-1} cluster of absorptions can be correlated with distortion of the carboxylate unit, specifically relaxation of the CO_2 angle and strengthening of the C-O bond.[55] Previous studies of carboxylato complexes suggest that an increased O-C-O angle leads to a larger splitting of the $\nu(CO)_{sym/asym}$ stretching bands,[61] a result that is in line with the behavior of the 1450 cm^{-1} cluster in $[Ru_2(O_2CMe)_4]_3[Cr(CN)_6]$. The latter displays mode softening on its low energy side ($\nu(CO)_{sym}$) and hardening of the high frequency component ($\nu(CO)_{asym}$). We attribute the unusual softening of the selective CH_3-related modes to weak electrostatic intermolecular interactions (for instance of the C-H$\cdots$O type) that strengthen with decreasing temperature.[62,63] Similar hydrogen-bonding-like interactions involving carboxylate oxygen are present in other diruthenium tetracarboxylates.[64] A closer look at the structure indicates plausible interactions between methyl groups of one sublattice and oxygen atoms of the other. Each methyl group has four short contacts to the neighboring oxygen with C$\cdots$O distances of 3.311 Å at 300 K. At 1.8 K, C$\cdots$O distances (3.264 Å) are shorter due to oxygen displacement towards the methyl groups. The latter subsequently affects Ru-O-C and C-O-C angles and the corresponding bond lengths.[55] Stronger intermolecular hydrogen-bonding may foster intersublattice interaction and overall structure stabilization.

IV. SUMMARY

Interest in the foundational aspects of multifunctionality is driving investigation of fundamental coupling mechanisms and structure-property relationships in molecule-based materials. Herein, we combine high field vibrational spectroscopies with an analysis of mode displacement patterns and trends to reveal the magnetoelastic coupling in $[Ru_2(O_2CMe)_4]_3[Cr(CN)_6]$. We find that high magnetic field competes with exchange interactions and distorts the $[Cr(CN)_6]^{3-}$ ion. Systematic changes in ν(CN) and the Cr-containing phonons provides evidence for overall $[Cr(CN)_6]^{3-}$ flexibility and, more specifically, an isotropically compressed CrC_6 octahedron. The magnetic intersublattice coalescence transition at $B_c \simeq 0.08$ T, by contrast, takes place without substantial spin-lattice interactions. Variable temperature spectroscopy reinforces the finding of an adaptable chromium environment that strengthens at low temperature. The understanding of magnetoelastic coupling in $[Ru_2(O_2CMe)_4]_3[Cr(CN)_6]$ provides insight into other chromium-containing materials where spin-lattice interactions contribute to ground state stabilization.[19,20,65] Moreover, distinctions between elastic vs. rigid molecular units and adaptable vs. static crystal environments are useful where building block choices figure into the design and control of materials for technological applications.[48,66]

ACKNOWLEDGEMENTS

Research supported by the National Science Foundation under DMR-1063880 (JLM), DMR-11063630 (JSM), DMR-0654118 (NHMFL), and by the U.S. Department Energy (NHMFL) and the State of Florida (NHMFL). We thank Randy Fishman for useful discussions.

* Present address: Department of Physics and Astrophysics, University of North Dakota, Grand Forks, North Dakota 58202.

[1] S. J. Blundell and F. L. Pratt, J. Phys.: Condens. Matter **16**, R771 (2004).
[2] E. Coronado and P. Day, Chem. Rev. **104**, 5419 (2004).
[3] J. S. Miller, A. J. Epstein, Angew. Chem. Int. Ed. Engl. **33**, 385 (1994); J. S. Miller, Chem. Soc. Rev. **40**, 3266 (2011).
[4] I. Ratera and J. Veciana, Chem. Soc. Rev. **41**, 303 (2012).
[5] X. -Y. Wang, C. Avendaño, K. R. Dunbar, Chem. Soc. Rev. **40**, 3213 (2011).
[6] J. Ribas-Ariño, J. J. Novoa, J. S. Miller J. Mater. Chem. **16**, 2600 (2006).
[7] M. Ohba, W. Kaneko, S. Kitagawa, T. Maeda, M. Mito, J. Am. Chem. Soc. **130**, 4475 (2008).
[8] J. L. Musfeldt, L. I. Vergara, T. V. Brinzari, C. Lee, L. C. Tung, J. Kang, Y. J. Wang, J. A. Schlueter, J. L. Manson, M. -H. Whangbo, Phys. Rev. Lett. **103**, 157401 (2009).
[9] M. Zentková, Z. Arnold, J. Kamarád, V. Kavečanský, M. Lukáčova, S. Mat'aš, M. Mihalik, M. Mitróová, A. Zentko, J. Phys.: Condens. Matter **19**, 266217 (2007).
[10] W. W. Shum, J. -H. Her, P. W. Stephens, Y. Lee, J. S. Miller, Adv. Mater. **19**, 2910 (2007).
[11] M. Verdaguer, A. Bleuzen, V. Marvaud, J. Vaissermann, M. Seuleiman, C. Desplanches, A. Scuiller, C. Train, R. Garde, G. Gelly, C. Lomenech, I. Rosenman, P. Veillet, C. Cartier, F. Villain, Coord. Chem. Rev. **190-192**, 1023 (1999); M. Verdaguer and G. S. Girolami, in *Magnetism: Molecules to Materials V*, edited by J. S. Miller, M. Drillon (Wiley-VCH, Weinheim, 2005), p. 283; K. Hashimoto and S. Ohkoshi, Phil. Trans. R. Soc. Lond. A **357**, 2977 (1999).
[12] T. E. Vos, Y. Liao, W. W. Shum, J. -H. Her, P. W. Stephens, W. M. Reiff, J. S. Miller, J. Am. Chem. Soc. **126**, 11630 (2004).
[13] J. S. Miller, T. E. Vos, W. W. Shum, Adv. Mater. **17**, 2251

(2005).
[14] W. W. Shum, J. N. Schaller, J. S. Miller, J. Phys. Chem. C **112**, 7936 (2008).
[15] R. S. Fishman, S. Okamoto, W. W. Shum, J. S. Miller, Phys. Rev. B **80**, 064401 (2009); R. S. Fishman and J. S. Miller, *ibid.* **83**, 094433 (2011).
[16] Y. Liao, W. W. Shum, J. S. Miller, J. Am. Chem. Soc. **124**, 9336 (2002).
[17] $[Ru_2(O_2CMe)_4]^+$ has an electronic configuration of $\sigma^2\pi^4\delta^2\pi^{*2}\delta^{*1}$ with a $^4B_{2u}$ ground state (Ref. [12] and references therein). Cr^{III} center in $[Cr(CN)_6]^{3-}$ possesses a ^4A_g ground state.
[18] R. S. Fishman, W. W. Shum, J. S. Miller, Phys. Rev. B **81**, 172407 (2010).
[19] M. Matsuda, C. de la Cruz, H. Yoshida, M. Isobe, R. S. Fishman, Phys. Rev. B **85**, 144407 (2012).
[20] H. Ueda, H. A. Katori, H. Mitamura, T. Goto, H. Takagi, Phys. Rev. Lett. **94**, 047202 (2005).
[21] P. A. Goddard, J. Singleton, P. Sengupta, R. D. McDonald, T. Lancaster, S. J. Blundell, F. L. Pratt, S. Cox, N. Harrison, J. L., Manson, H. I. Southerland, J. A. Schlueter, New J. Phys. **10**, 083025 (2008).
[22] B. S. Kennon, K. H. Stone, P. W. Stephens, J. S. Miller, CrystEngComm. **11**, 2185 (2009).
[23] We attribute the observed phonon response to magnetic field as due to local lattice distortions rather than spin-phonon coupling.
[24] L. H. Jones, Inorg. Chem. **2**, 777 (1963); L. H. Jones, M. N. Memering, B. I. Swanson, J. Chem. Phys. **54**, 4666 (1971).
[25] I. Nakagawa and T. Shimanouchi, Spectrochim. Acta A **26**, 131 (1970); I. Nakagawa, Bull. Chem. Soc. Jpn. **46**, 3690 (1973).
[26] O. Zakharieva-Pencheva and V. A. Demetiev, J. Mol. Struct. **90**, 241 (1982).
[27] S. -K. Park, C. -K. Lee, S. -H. Lee, N. -S. Lee, Bull. Korean Chem. Soc. **23**, 253 (2002).
[28] Cr-C stretch and Cr-C-N bend are considered to be mixed with each other and present to some degree in each vibration.
[29] V. M. Miskowski, T. M. Loehr, H. B. Gray, Inorg. Chem. **26**, 1098 (1987).
[30] The second component of ν(Ru-O) is expected near 340 cm^{-1} (which overlaps with the ν(Cr-C) band) and probably corresponds to the weak feature near 345 cm^{-1}.[29] This peak displays a very weak temperature dependence (<1 cm^{-1}), and no field dependence within our error bars, a behavior that is quite similar to the 400 cm^{-1} feature, thus providing an additional support to its assignment.
[31] At this moment location of the ν(Ru-N) stretch is uncertain. Feature near 280 cm^{-1} likely corresponds to one of the expected (RuO) deformation bands of weak intensity, while peaks near 620 and higher energy 690 cm^{-1} are assigned to ρ(COO) rocking and δ(COO) bend, respectively. Very weak excitation near 945 cm^{-1} corresponds to ν(C-C) stretch.[29,59,60] None of these bands display sensitivity to magnetic field even in highly concentrated samples.
[32] C. M. Hartwig, E. Wiener-Avnear, S. P. S. Porto, Phys. Rev. B **5**, 79 (1972).
[33] J. L. Musfeldt, K. Kamarás, and D. B. Tanner, Phys. Rev. B. **45**, 10197 (1992).
[34] X. S. Xu, J. de Groot, Q. -C. Sun, B. C. Sales, D. Mandrus, M. Angst, A. P. Litvinchuk, J. L. Musfeldt, Phys. Rev. B **82**, 014304 (2010).
[35] M. Kim, X. M. Chen, Y. I. Joe, E. Fradkin, P. Abbamonte, S. L. Cooper, Phys. Rev. Lett. **104**, 136402 (2010).
[36] T. V. Brinzari, P. Chen, Q. -C. Sun, J. Liu, L. C. Tung, Y. J. Wang, J. Singleton, J. A. Schlueter, J. L. Manson, M. -H. Whangbo, A. P. Litvinchuk, J. L. Musfeldt, *in preparation*
[37] Small frequency shifts are sometimes difficult to discern, making $\Delta\alpha$ a more sensitive parameter (Supplemental Material). We carried out this analysis for all the phonons, including the 120 cm^{-1} feature for comparison.
[38] A. Marvilliers, S. Parsons, E. Rivière, J. -P. Audière, M. Kurmoo, T. Mallah, Eur. J. Inorg. Chem. 1287 (2001).
[39] G. Lazari, T. C. Stamatatos, C. P. Raptopoulou, V. Psycharis, M. Pissas, S. P. Perlepes, A. K. Boudalis. Dalton Trans. 3215, (2009).
[40] D. Zhang, H. Wang, Y. Chen, Z. -H. Ni, L. Tian, J. Jiang, Inorg. Chem. **48**, 11215 (2009).
[41] E. Granado, A. García, J. A. Sanjurjo, C. Rettori, I. Torriani, F. Prado, R. D. Sánchez, A. Caneiro, S. B. Oseroff, Phys. Rev. B **60**, 11879 (1999).
[42] Anisotropy associated with crystal field effects is absent for Cr^{III} sites.
[43] Y. Narumi, N. Terada, Y. Tanaka, M. Iwaki, K. Katsumata, K. Kindo, H. Kageyama, Y. Ueda, H. Toyokawa, T. Ishikawa, H. Kitamura, J. Phys. Soc. Jpn. **78**, 043702 (2009).
[44] F. D. Hardcastle and I. E. Wachs, J. Raman Spectrosc. **21**, 683 (1990).
[45] D. Cremer, A. Wu, A. Larsson, E. Kraka, J. Mol. Model. **6**, 396 (2000).
[46] The weak structure on the left hand side of the 360 cm^{-1} peak in $\Delta\alpha$ is beyond our sensitivity. Higher magnetic fields (>35 T) may reveal its behavior and any signatures of octahedral distortion.
[47] S. M. Holmes and G. S. Girolami, J. Am. Chem. Soc. **121**, 5593 (1999).
[48] D. R. Talham and M. W. Meisel, Chem. Soc. Rev. **40**, 3356 (2011).
[49] Ø. Hatlevik, W. E. Buschmann, J. Zhang, J. L. Manson, J. S. Miller, Adv. Mater. **11**, 914 (1999).
[50] O. Sato, T. Iyoda, A. Fujishima, K . Hashimoto, Science **272**, 704 (1996).
[51] W. Kosaka, K. Nomura, K. Hashimoto, S. Ohkoshi, J. Am. Chem. Soc. **127**, 8590 (2005).
[52] M. G. Hilfiger, M. Chen, T. V. Brinzari, T. M. Nocera, M. Shatruk, D. T. Petasis, J. L. Musfeldt, C. Achim, K. R. Dunbar, Angew. Chem. Int. Ed. **49**, 1410 (2010).
[53] P. Chen, N. Lee, S. McGill, S. -W. Cheong, J. L. Musfeldt, Phys. Rev. B **85**, 174413 (2012).
[54] *Magnetism: fundamentals*, edited by E. du Trémolet de Lacheisserie, D. Gignoux, M. Schlenker (Springer Science, Boston, 2005).
[55] R. S. Fishman, J. Campo, T. E. Vos, J. S. Miller, *Submitted* Phys. Rev. B.
[56] I. Loa, K. Syassen, R. K. Kremer, Solid State Commun. **112**, 681 (1999); Z. V. Popović, V. Stergiou, Y. S. Raptis, M. J. Konstantinović, M. Isobe, Y. Ueda, V. V. Moshchalkov, J. Phys.: Condens. Matter **14**, L583 (2002).
[57] K. Ishida and F. C. Hawthorne, Am. Mineral. **96**, 566 (2011).
[58] The frequency shift of >5 cm^{-1} is observed for some peaks on the low energy side of the 1450 cm^{-1} cluster and >10 cm^{-1} for the component on the high energy part. The exact position of peaks are hard to track above $\simeq$100 K due to their strong overlap.
[59] A. M. Heyns, J. Mol. Structure, **11**, 93, (1972).

[60] Y. Mathey, D. R. Greig, D. F. Shriver, Inorg. Chem. **21**, 3409 (1982).
[61] G. B. Deacon and R. J. Phillips, Coord. Chem. Rev. **33**, 227 (1980).
[62] S. Brown, J. Cao, J. L. Musfeldt, M. M. Conner, A. C. McConnell, H. I. Southerland, J. L. Manson, J. A. Schlueter, M. D. Phillips, M. M. Turnbull, C. P. Landee, Inorg. Chem. **46**, 8577, (2007).
[63] T. V. Brinzari, C. Tian, G. J. Halder, J. L. Musfeldt, M. -H. Whangbo, J. A. Schlueter, Inorg. Chem. **48**, 7650 (2009).
[64] M. A. S. Aquino, Coord. Chem. Rev. **248**, 1025 (2004).
[65] K. Penc, N. Shannon, H. Shiba, Phys. Rev. Lett. **93**, 197203 (2004).
[66] H. Tokoro and S. Ohkoshi, Dalton Trans. **40**, 6825 (2011).